JOURNAL OF CATALYSIS 148, 540–549 (1994)

A Kinetic Investigation of Co-Solvent Effects in Oxyfunctionalization of *n*-Hexane by Hydrogen Peroxide on TS-2

H. Fu and S. Kaliaguine[1]

Département de Génie Chimique and CERPIC, Université Laval, Ste-Foy, Québec, Canada

Received October 19, 1993; revised February 23, 1994

Systematic experiments of *n*-hexane conversion to *n*-hexanol and *n*-hexanone by hydrogen peroxide in the presence of TS-2, in absence as well as in presence of a co-solvent, were performed. Methanol, acetone, and acetonitrile were used. The reaction was monitored by GC analysis of the organic phase and by measurements of the volume of the oxygen evolved as a function of time. Iodometric titration of hydrogen peroxide was performed at the end of the 5-h test. Independent measurements of the *n*-hexane solubility equilibrium were also performed. The catalyst was characterized by AA, XRD, FTIR, and UV–visible spectroscopy. These data allowed a kinetic analysis of the initial rates of oxidation on the secondary carbons (*n*-hexane-2ol and -3ol) and a kinetic model is proposed for these two reactions, yielding the following rate equation:

$$r_{i0} = k_i[H_2O_2]^2/\{1 + K[H_2O_2]/[\text{Solvent}]\} \quad (i = 1, 2).$$

When applied to rates measurement free of pore diffusion limitations, this model suggests that the active site can accommodate two H_2O_2 molecules which is discussed in light of the Ti environment in TS-2 proposed recently by Trong On *et al.* (*Catal. Letter* 16, 85 (1992) and *J. Mol. Catal.* 74, 233 (1992)). The rate of the parallel reaction of H_2O_2 decomposition is shown to be of first order with respect to the concentration of hydrogen peroxide:

$$r_3 = k_3[H_2O_2].$$

The effect of the co-solvent on initial rates of alcohol formation and secondary oxidation to ketones is discussed.

INTRODUCTION

The introduction of oxygen containing functional groups in alkanes was carried out more than two decades ago by Fripiat and co-workers (1), using molecular oxygen at 160°C and 25 atm. Different types of catalysts were used such as homogeneous catalysts, Mn, Ni, Co-exchanged Zeolite 13X, and transition metals supported by Al_2O_3. In this approach, *n*-hexane is essentially oxidized into acetic acid and minor amounts of C_6 alcohols and ketones. It was reported (2) that the cleavage of carbon–carbon bonds in the presence of transition metal complexes leads mainly to oxidation to acids. Oxyfunctionalization without C–C bond cleavage catalyzed by a ruthenium heteropolyanion ($SiRu(H_2O)W_{11}O_{39}^{5-}$) in liquid phase with various primary oxidants including potassium persulphate, sodium periodate, *t*-butyl hydroperoxide, and iodosylbenzene has also been achieved (3, 4). Ten years ago, the discovery of titanium silicalite-1 (TS-1) opened up new opportunities (5). It was soon established that TS-1 was a very efficient catalyst for various oxidations with hydrogen peroxide under very mild conditions, such as hydroxylation of aromatics (6–9), expoxidation of olefins (10, 11), diolefins (5), and allylic compounds (12), and oxidation of alcohols to aldehydes and ketones (13). The first commercial process utilizing TS-1 as a catalyst was introduced by Enichem (Italy) for the hydroxylation of phenol to hydroquinone and catechol (14).

Recently, the direct oxidation of saturated hydrocarbons was reported, using TS-1 or TS-2 as catalysts and aqueous H_2O_2 as the oxidizing agent (15–17). Most of the published studies in this field (15–20) mainly dealt with the effect of various reaction conditions on conversion and product distribution. Although the mechanism of selective oxidation of alkanes catalyzed by TS-1 has been discussed (19, 20), it is still uncertain. No study of the reaction kinetics and mechanism over TS-1 and TS-2 is yet available in the literature. The objective of this paper is to examine the effect of co-solvents on the *n*-hexane partial oxidation over titanium silicalite TS-2. A kinetic analysis of this effect is performed and the reaction mechanism is discussed based on the analysis of initial rate data.

EXPERIMENTAL PROCEDURES

Synthesis of TS-2

Titanium silicalites (TS-2) were synthesized hydrothermally using the procedure described by Thangaraj *et al.* (21). Gels with different compositions were prepared by

[1] To whom correspondence should be addressed.

0021-9517/94 $6.00

mixing calculated amounts of tetraethyl orthosilicate, 2-propanol, tetrabutylammonium hydroxide (organic template 40% in water), and water. The commercial template (TBA-OH) was found to contain about 2000 ppm of Na. Therefore, sodium-free template was prepared by the classical method of reacting TPA-Br with freshly prepared silver oxide (22). Na impurities are known to favour the decomposition of H_2O_2 (23) in reaction conditions and to promote the formation of extraframework titanium silicate during the synthesis of titanium silicalites (24). The prepared gels were transferred to teflon-coated stainless-steel autoclaves and heated under autogenous pressure at 170°C for 7 days. The solids were then filtered, washed with deionized water, and dried at 100°C. The organic template was decomposed by calcination at 500°C.

Physicochemical Characterization

Infrared measurements were carried out using self-supporting wafers obtained by pressing mixtures of 2 mg of TS-2 and 100 mg of KBr. IR spectra were recorded in the range 4000–400 cm^{-1} with 2 cm^{-1} resolution, using a Digilab FTS-60 spectrometer.

The unit cell parameters and crystallinity were calculated from X-ray powder diffraction spectra using quartz as an internal reference, on a Philips spectrometer with PW 1010 generator and PW 1050, 0–2θ, computer-assisted goniometer.

The chemical analysis of the samples was performed by atomic absorption using a Perkin–Elmer 1100B spectrometer. The material was dissolved in (20% HF + 20% HCl) solutions at 60°C.

The BET surface area and micropore volume were determined by nitrogen adsorption using an OMNISORP-100 instrument at relative pressure $P/P^0 \leq 0.1$.

Particle size was determined using a JEOL 840-A scanning electron microscope equipped with an EDX analyzer.

The UV–vis reflectance spectra were performed with a Perkin–Elmer Lambda 5.

Reaction Conditions

n-Hexane 99 + % (20 g), co-solvents (0–31 g), and the catalyst (500 mg) were added to a 180-ml round-bottom pyrex reactor with a sampling port and a heating water jacket. This reactor is equipped with a magnetic stirrer and a reflux condenser and it is linked to an oxygen collector. In a typical experiment, when the reactor temperature reached 55°C, 10 g of aqueous solution of H_2O_2 (30%) was added and the reaction started.

At different times on stream reaction products were withdrawn from the organic phase through the sampling port. Analysis of these products was performed by gas chromatography using a DB Wax capillary column. The assumption that the fraction of oxygenates left in solution in the aqueous phase is negligible was tested experimentally by GC analyzing ether extracts from the aqueous phase. The error made was found to be less than 5% of the oxygenates in the organic phase (25). The volume of collected O_2 was recorded as a function of time on stream. At the end of the experiment, the concentration of H_2O_2 remaining in the reactor was determined by iodometric titration, which gave a double check of the hydrogen peroxide conversion.

Thermodynamics of Solubility

Solubility of *n*-hexane in water in the presence of the co-solvents was determined by equilibrating a hydrocarbon layer and a water layer. The equilibration flasks were maintained at constant temperature by immersion in a constant-temperature bath controlled to within ±0.1°C. The water layer was sampled periodically and analyzed by gas chromatography. After a time on the order of 5 days, the phase compositions had become constant, indicating that equilibrium was attained.

n-Hexane (99 + %), methanol (99.9 + %, HPLC grade), acetone, and acetonitrile (HPLC grade) were obtained from Aldrich Chemical Co., and were used without further purification. Analysis of the aqueous layer was done by injection of samples into a Hewlett–Packard 5890 gas chromatograph equipped with a flame ionization detector and an automatic integrator. The column used was DB Wax.

In these reaction systems, there are two liquid phases even under vigorous stir. At rest, the organic phase is upper, whereas the aqueous phase is below and contains H_2O_2, the co-solvent, a small amount of dissolved *n*-hexane, and the catalyst TS-2. It is considered that the reaction takes place in the aqueous phase. A series of experiments were carried out to measure the volume of the aqueous phase. Mixtures of 20 g of *n*-hexane, 10 g of H_2O_2 solution, and the corresponding amounts (0–31 g) of co-solvents (methanol, acetone, acetonitrile, and water) were laid off in a burette overnight before the volumes of the two phases were measured.

RESULTS AND DISCUSSION

Equilibrium of Solubility

n-Hexane solubility in water is an important feature of the reaction medium because the concentration of *n*-hexane in the aqueous phase is a priori likely to be a kinetic parameter. The objective of this part of the study is to examine the effects of the co-solvent used in the kinetic experiments (namely methanol, acetone, and acetonitrile) on the solubility of *n*-hexane in water in conditions close to those prevailing in the reaction medium.

Thus *n*-hexane and the aqueous phase were mixed in the same proportions as in the reaction tests and the same amounts of co-solvent were also added. Table 1 reports the values of the measured equilibrium *n*-hexane concentrations in the aqueous phase. From this table it appears that for co-solvent addition of 1 to 8 g moderate increases in *n*-hexane solubility are observed compared to the co-solvent free system. For the highest co-solvent content (31 g), however, this increase is very significant, which should allow a good test of the effect of *n*-hexane concentration on reaction rates.

The data reported in Table 1 have been found to be in reasonable agreement with the *n*-hexane solubility data in the literature (25–28).

Catalyst Characterization

All catalytic tests reported were performed in the presence of samples of Ti-silicalite from the same synthesis batch. This material will simply be designated below as TS-2.

The framework IR spectrum of TS-2 shows a characteristic adsorption at 960 cm^{-1}, which is consistent with what has been reported in the literature (21). According to XRD analysis, TS-2 contains a MEL phase of good crystallinity. No extra zeolitic crystalline or amorphous phase were detected by XRD. SEM analysis showed that

TABLE 1

n-Hexane Solubility in Aqueous Phase in the Presence of Co-Solvents at 55°C

Co-solvent		
Dipole moment (Debye)	Mass added (g)	*n*-Hexane in aqueous phase (mg/liter)
Water (1.87)	0	13
Methanol (1.70)	1	14
	3	16
	5	17
	8	26
	31	437.5
Acetone (2.88)	1	15
	3	16
	5	17
	8	20
	31	18,000
Acetonitrile (3.92)	1	13
	3	16
	5	18
	8	99
	31	5,300

Note. Conditions: laid off time 5 days, 55°C; *n*-hexane, 20 g; H_2O, 10 g; various amounts of co-solvent.

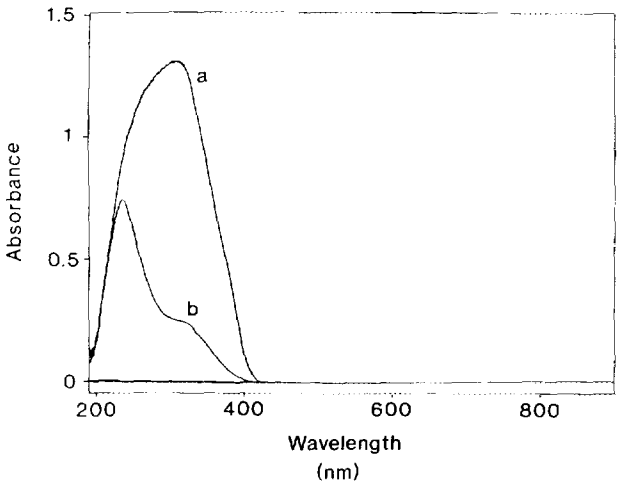

FIG. 1. UV–vis diffuse reflectance spectra of (a) anatase and (b) TS-2.

the sample consists of elongated crystallites of uniform size with an average width of 0.2 μm and a length to width aspect ratio of 4.5. The BET surface area of TS-2 is 556 m^2/g (measured at $0.006 \leq P/P_0 < 0.1$). The atomic ratios of Ti/(Ti + Si) and Na/Ti were determined by atomic adsorption to be 1.41 and 0.19%, respectively. Figure 1 depicts the diffuse reflectance spectra of TS-2 and crystalline TiO_2 (anatase). The strong transition at 220 nm observed on TS-2 is undoubtedly associated with an electronic transition localized on structures containing titanium in tetrahedral coordination.

n-Hexane Oxyfunctionalization

GC analysis showed that the main products of the reaction were 2- and 3-hexanol and 2- and 3-hexanone. Notably, 1-hexanol and hexanal were not detected. The partial oxidation of *n*-hexane may therefore be described by the following scheme:

$$H_2O_2 + nC_6H_{14} \xrightarrow[[1]]{} \text{2-hexanol} \xrightarrow[[4]]{H_2O_2} \text{2-hexanone}$$

$$H_2O_2 + nC_6H_{14} \xrightarrow[[2]]{} \text{3-hexanol} \xrightarrow[[5]]{H_2O_2} \text{3-hexanone}$$

$$H_2O_2 \xrightarrow[[3]]{} H_2O + \tfrac{1}{2}O_2.$$

Designating the partial conversions of H_2O_2 through the three parallel routes as x_1, x_2, and x_3, respectively, the total H_2O_2 conversion is $x = x_1 + x_2 + x_3$. The selectivity for oxygenates production is defined as $y = (x_1 + x_2)/x$, where x_1 and x_2 are given by

$$x_1 = (N_{2OL} + 2N_{2ONE})/N^0_{H_2O_2}$$

$$x_2 = (N_{3OL} + 2N_{3ONE})/N^0_{H_2O_2},$$

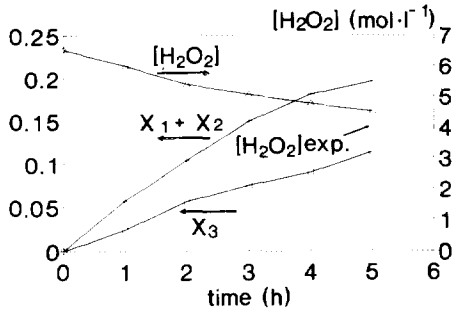

FIG. 2. Hydrogen peroxide concentration in aqueous phase and partial conversion. Reaction conditions: temperature, 55°C; TS-2, 500 mg; H_2O_2, 0.08 mol; *n*-hexane, 20 g; methanol, 3 g.

$N^0_{H_2O_2}$ being the initial number of H_2O_2 moles in the reactor.

Figure 2 reports the H_2O_2 concentration in the aqueous phase and the H_2O_2 partial conversion as functions of the reaction time for a typical experiment. The x_3 data are calculated from the measured volumes of gaseous oxygen collected, whereas $(x_1 + x_2)$ is derived from the measured concentration of the four oxygenates. The H_2O_2 concentration values are back calculated as $C_0(1 - x)$. The comparison with the experimental value obtained by iodometric titration at the end of the 5-h experiment is satisfactory and indicates that both values differ by 5–8%. Thus the calculations based on material balance are considered reliable.

Table 2 gives conversions and selectivity data obtained in all experiments after 5 h reaction time. The *n*-hexane conversion is calculated as $x' = x'_1 + x'_2$, where $x'_1 = (N_{2OL} + N_{2ONE})/N^0_{C6}$ and $x'_2 = (N_{3OL} + N_{3ONE})/N^0_{C6}$ where N^0_{C6} is the initial number of moles of *n*-hexane in the reactor.

The H_2O_2 conversion data listed in Table 2 are calculated from the H_2O_2 concentration in aqueous phase value measured at the end of each experiment. The H_2O_2 selectivity is the selectivity to oxygenates (y) at the end of the run. The next columns give the product distribution, the OL/ONE ratio defined as $(N_{2OL} + N_{3OL})/(N_{2ONE} + N_{3ONE})$, and the 2- /3- ratio defined as $(N_{2OL} + N_{2ONE})/(N_{3OL} + N_{3ONE})$.

The effects of the nature and content of the co-solvent are best described in Fig. 3. This figure indicates that the 2- /3- ratio is higher than 1 only with methanol as co-solvent and that in this case this ratio increases with CH_3OH concentration. Thus methanol favours the C-2 oxidation. With addition of water the 2- /3- ratio remains

TABLE 2

The Influence of Co-solvents on the Conversion and Product Selectivities

Co-solvent	(g)	*n*-C_6 conversion (%)	H_2O_2 (%)		Product distribution (mol. %)				OL/ONE ratio	2- /3- ratio
			Conv. (%)	Sel. (%)	2OL	2ONE	3OL	3ONE		
CH_3OH	1	3.6	27.1	59.1	4.2	46.3	28	21.5	0.48	1.02
	3	4.4	31	63.3	3.3	48.5	28.2	20	0.48	1.02
	5	3.8	24.8	69.6	2.4	51.6	27	19.1	0.42	1.17
	8	3.1	19.6	70	4	53.4	27.6	15	0.46	1.35
	31	0.5	3.7	52.1	23.7	39.2	33.5	3.6	1.34	1.70
H_2O	0	1.7	20.3	27.5	7	37.8	35.3	19.9	0.73	0.81
	1	1.4	23.1	26	8.1	36	33.5	22.4	0.71	0.79
	3	1.3	20.6	24.1	8.3	36.6	31.9	23.2	0.67	0.81
	5	1.2	24.5	21.4	9.9	38.1	29.9	22.2	0.66	0.92
	8	1.0	20.7	21	8.9	39.9	25.3	25.9	0.52	0.95
	31	0.2	14.5	34.1	10.9	38.4	32.6	18.2	0.79	0.97
C_3H_6O	1	2.1	22.1	40.8	8.2	41.8	35.3	14.7	0.77	1.0
	3	2.2	24.3	44.4	9.5	38.4	41.6	10.5	1.05	0.92
	5	2.5	11.2	84.5	12	32.7	46.8	8.6	1.42	0.81
	8	2.0	9.8	75.4	16.7	25.9	50.7	6.7	2.07	0.74
	31	0.5	2.6	53.5	28.6	6.4	62.8	2.2	10.7	0.54
CH_3CN	1	1.5	10.3	50	10.5	8.6	61.5	19.4	2.57	0.24
	3	1.5	11.7	40.4	10.8	4.7	68.9	15.6	3.93	0.18
	5	1.2	14.3	27.8	10.6	4.2	70.9	14.4	4.38	0.17
	8	1.0	11.7	24.9	11	2.8	76	10.1	6.74	0.16
	31	0.3	7.8	13	10.6	3.8	80	6.0	9.25	0.17

Note. Reaction conditions: Temp., 55°C; Reaction time, 5 h; TS-2, 500 mg; *n*-hexane (mol): H_2O_2 (mol): 2.7.

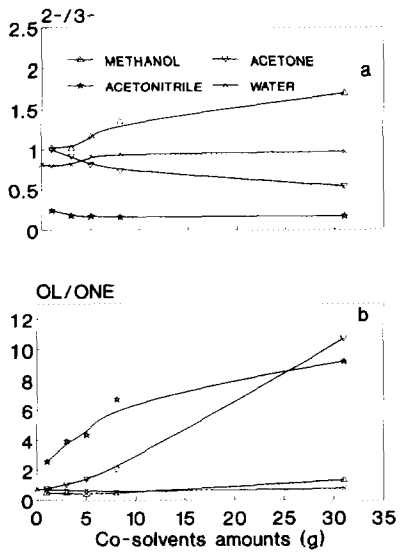

FIG. 3. The ratio of 2- /3- and OL/ONE versus co-solvent amount. Reaction conditions: temperature, 55°C; reaction time, 5 h; TS-2, 500 mg; H_2O_2, 0.08 mol; *n*-hexane, 20 g; co-solvent, 1–31 g.

close to 1, but acetone and even more acetonitrile favour the C-3 oxidation, since 2- /3- is clearly lower than 1 in this case.

A continuous increase in the OL/ONE ratio is observed upon addition of acetone and acetonitrile. This obviously indicates that these two co-solvents decrease the relative rate of secondary oxidation to ketones with respect to the primary alcohol formation. It is interesting to note that the order for the OL/ONE ratio, which is

$$CH_3OH \lesssim H_2O < C_3H_6O \lesssim CH_3CN$$

is also the order of the dipole moment of these solvents (see Table 1). One possible explanation for such an effect is as follows: more polar solvents, which will solvate more efficiently the *n*-hexanol molecules, may affect the solubility of these molecules in such a way that the *n*-hexanol would be prevented from secondary oxidation through its more efficient transfer to the organic phase.

Reaction Rate Data

In order to estimate initial rates for reactions [1] and [2] (r_{10} and r_{20}) graphs similar to those shown in Fig. 4 were drawn. These show the variations of (N_{2OL} + N_{2ONE}) and (N_{3OL} + N_{3ONE}) as functions of reaction time. As seen on the curves of a typical experiment reported in Fig. 4, the initial slopes (which are numerical estimates of r_{10} and r_{20}) are well approximated by the slope of the segments joining points at times 0 and 1 h. All estimates of initial rates r_{10} and r_{20} are listed in Table 3. These values are expressed in mole per hour for the same mass (500 mg) of the same catalyst.

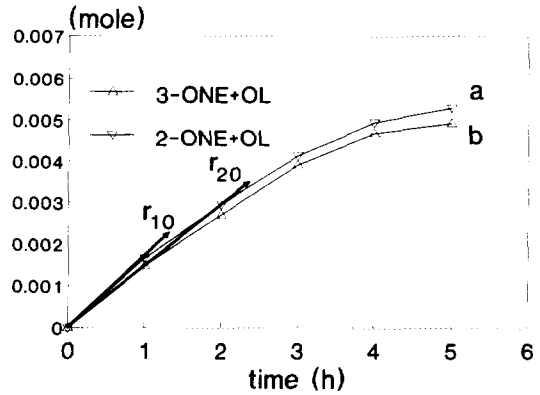

FIG. 4. Influence of duration of run on 2OL + ONE and 3OL + ONE production. Reaction conditions are as in Fig. 2.

The rate of oxygen evolution is a measure of the H_2O_2 decomposition rate through reaction [3], r_3. Figure 5 shows a series of curves for the volume of oxygen collected as a function of reaction time. This particular series is for the set of experiments using methanol as the co-solvent. It is interesting to note that for reaction time below 2 h low rates are observed. This effect is associated to the necessary saturation of the reaction medium and the water in the gas collector, before the oxygen produced can evolve to the gas phase. Thus only oxygen evolution rates at times higher than 2 h were used as measurements

TABLE 3

Initial Rate Measurements at 55°C

Co-solvent (g)		r_{10} (mol h^{-1})	r_{20} (mol h^{-1})
Methanol	1	1.38×10^{-3}	1.31×10^{-3}
	3	1.66×10^{-3}	1.48×10^{-3}
	5	1.40×10^{-3}	1.35×10^{-3}
	8	9.50×10^{-4}	6.48×10^{-4}
	31	1.24×10^{-4}	9.50×10^{-5}
Water	0	7.41×10^{-4}	8.47×10^{-4}
	1	5.87×10^{-4}	6.66×10^{-4}
	3	3.61×10^{-4}	4.77×10^{-4}
	5	3.16×10^{-4}	3.58×10^{-4}
	8	1.55×10^{-4}	1.98×10^{-4}
	31	1.14×10^{-4}	1.28×10^{-4}
Acetone	1	9.49×10^{-4}	1.03×10^{-3}
	3	9.60×10^{-4}	1.26×10^{-3}
	5	7.89×10^{-4}	1.20×10^{-3}
	8	4.64×10^{-4}	8.22×10^{-4}
	31	1.55×10^{-4}	2.24×10^{-4}
Acetonitrile	1	2.75×10^{-4}	1.21×10^{-3}
	3	2.00×10^{-4}	1.04×10^{-3}
	5	1.60×10^{-4}	9.07×10^{-4}
	8	1.08×10^{-4}	6.02×10^{-4}
	31	3.30×10^{-5}	1.76×10^{-4}

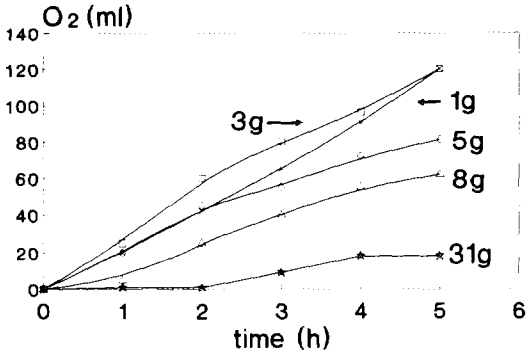

FIG. 5. Volume of O_2 collected as a function of reaction time. Reaction conditions are as in Fig. 2.

of H_2O_2 decomposition rates. The rate values obtained from the data shown in Fig. 5 are reported in Fig. 6, which shows that this rate may be roughly considered as first order.

Kinetic Model

A systematic effort of kinetic model derivation using the Langmuir–Hinshelwood formalism was conducted and kinetic equations for initial rates were obtained for a large series of mechanistic hypotheses. The equations were tested for the rate data reported in Table 3 as functions of initial H_2O_2 concentration in the aqueous phase and of estimates of *n*-hexane concentrations from the equilibrium data reported in Table 1. Two conclusions resulted from this study. First, the initial rate data are not correlated with the *n*-hexane concentration in the aqueous phase. Second, the following mechanism allows a reasonable representation of all the kinetic data in Table 3.

H_2O_2 adsorption: $\quad B + I \rightleftharpoons BI$ [6]

$\quad B + BI \rightleftharpoons BBI.$ [7]

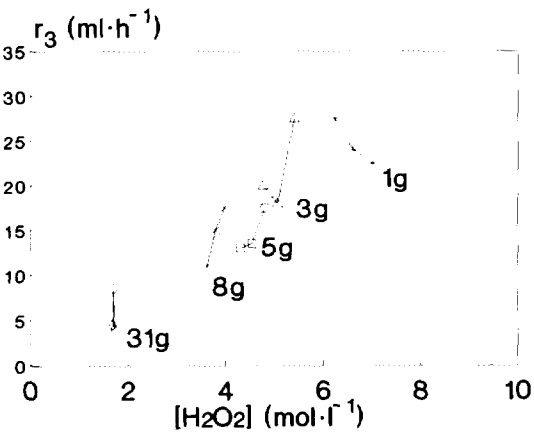

FIG. 6. Rate of H_2O_2 decomposition. Reaction conditions are as in Fig. 2.

Reaction: $\quad A + BBI \rightleftharpoons EI.$ [8]

Product desorption: $\quad EI \rightleftharpoons P + BI.$ [9]

In these equations I stands for a bare site on the catalyst surface, A, B, and P stand respectively for free *n*-hexane, H_2O_2, and *n*-hexanol molecules in the aqueous phase, and BI, BBI, and EI stand for surface complexes.

A satisfactory rate equation is obtained when assuming that step [7] is rate limiting. In this case the rate expression is

$$r_i = \frac{k_i([B]^2 - [P][B]/K[A])}{1 + K_1[B] + (K_2[P][B]/K[A]) + K_3[P][B]} \quad [10]$$

and at time zero when all product concentrations are zero, where r_{i0} is the initial rate of hexanol formation,

$$r_{i0} = k_i \frac{[B]^2}{1 + K_1[B]} \quad (i = 1, 2). \quad [11]$$

When $K_1[B] \ll 1$, Eq. [11] becomes

$$r_{i0} = k_i[B]^2 \quad (i = 1, 2), \quad [12]$$

Kinetic Data Fitting

First, the proposed kinetic model had been checked by fitting experimental data with the simplified Eq. [12]. The value of k_i is obtained by plotting r_{i0} versus $[B]^2$. For acetonitrile and water the data fitting is satisfactory. There is, however, a large deviation to Eq. [12] at the higher H_2O_2 concentrations in the presence of methanol and acetone (see Fig. 7). It was thus necessary to use Eq. [11] in order to fit these data. Moreover, as K_1, which is the equilibrium constant in Eq. [6], is obviously a function of the co-solvent concentration, it was written as

$$K_1 = \frac{K_s}{[S]}, \quad [13]$$

where [S] stands for the co-solvent concentration in the aqueous phase.

Thus k_i and K_s may be estimated by linear regression of the linearized form of Eq. [11],

$$k_i \frac{[H_2O_2]^2}{r_{i0}} = 1 + K_s \frac{[H_2O_2]}{[S]}, \quad [14]$$

which yields

$$r_{i0} = k_i \frac{[H_2O_2]^2}{1 + K_s([H_2O_2]/[S])}. \quad [15]$$

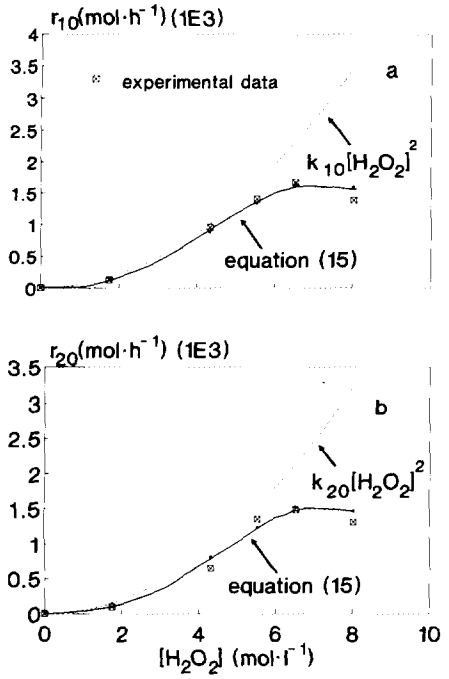

FIG. 7. Initial rate for 2OL or 3OL formation as a function of H_2O_2 concentration. Co-solvent methanol.

Examples of fitting results for methanol and water are shown in Figs. 7 and 8, respectively. The dashed line represents Eq. [12]. The solid line was drawn based on Eq. [15]. It can be seen that the predictions based on Eq. [15] (solid lines in Fig. 7) closely fit the experimental data. The fitting parameters K_s and k_i for different co-solvents are listed in Table 4. The correlation coefficient indicated as R square is also listed in Table 4.

It is important to know whether or not *n*-hexane oxidation is restricted by pore diffusion limitation as was the case in the work of van der Pol *et al.* (29) on the hydroxylation of phenol on TS-1. A method to describe the influence of internal diffusion on the observed reaction rate is given by the Weisz modulus (Φ) and catalyst effectiveness factor (η) (30), which can be expressed as

$$\Phi = \frac{(p/6)^2 R_0}{D_{\text{eff}} C_0} \quad [16]$$

$$\eta = \frac{\tanh(\phi)}{\phi} \quad [17]$$

$$\Phi = (\phi)^2 \eta, \quad [18]$$

where p is the mean diffusion length (m), R_0 is the observed *n*-hexane consumption rate per unit volume of catalyst (mol/m^{3}s), D_{eff} is the effective diffusion coefficient of *n*-hexane (m^2/s), C_0 is the concentration of *n*-hexane at the outer surface of the catalyst (mol/m^3), η is the catalyst effectiveness factor, ϕ is the Thiele modulus.

For the calculation of the value of the Weisz modulus the values of the reaction rate R_0, the average length of the diffusion path p, and the *n*-hexane concentration at the outer surface of the catalyst particles C_0 are our experimental measurements. D_{eff} was estimated from the experimental work of Wu *et al.* (31). This is of course a crude estimate, as their data are for self-diffusion of *n*-hexane in silicalite-1, which we interpolated at a temperature of 55°C. The calculated values of Φ, ϕ, and η are reported in Table 5. It is especially interesting to note that the experiments in which η is clearly lower than one (say $\eta < 0.80$) are also the ones in which r_{10} and r_{20} are lower than the predictions of Eq. [12]. It is the presence of these

TABLE 4

Estimated Values for the Parameters in Eq. [15] at 55°C

		k_i (ml^2 mol^{-1} h^{-1})		R Square	
	K_s	1	2	1	2
Methanol	0.43	54.2	50.1	0.99	0.98
Acetone	0.12	25.0	36.7	0.99	0.99
Acetonitrile	0	4.5	22.0	0.97	0.90
Water	0	9.8	11.4	0.97	0.98

Note. i = 1 stands for the reaction on C-2 yielding 2-hexanol; i = 2 stands for C-3 producing 3-hexanol.

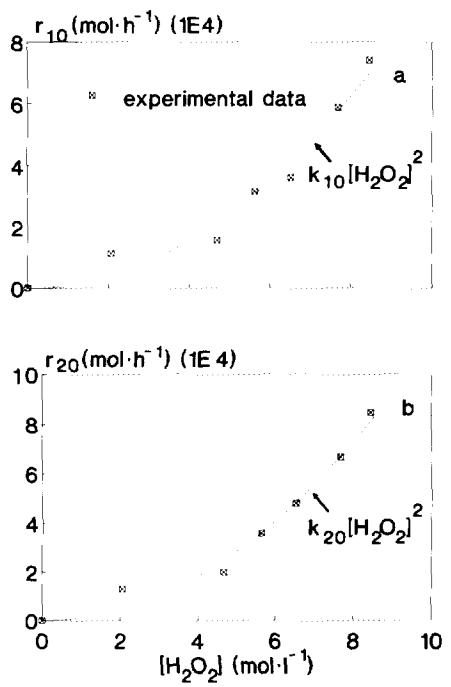

FIG. 8. Initial rate for 2OL or 3OL formation as a function of H_2O_2 concentration. Co-solvent water.

TABLE 5

Weisz Modulus Φ, Thiele Modulus ϕ, and Catalyst Effectiveness Factor η

Co-solvent	(g)	Φ	ϕ	η
Methanol	1	0.82	1.04	0.75
	3	0.84	1.06	0.74
	5	0.69	0.94	0.78
	8	0.26	0.54	0.91
	31	0.0022	0.05	1.00
Acetone	1	1.03	1.21	0.69
	3	1.08	1.25	0.68
	5	0.91	1.11	0.72
	8	0.50	0.77	0.84
	31	0.00016	0.01	1.00
Acetonitrile	1	0.63	0.88	0.80
	3	0.42	0.70	0.86
	5	0.32	0.60	0.89
	8	0.04	0.19	0.99
	31	0.0002	0.02	1.00
Water	0	0.29	0.57	0.90
	1	0.23	0.50	0.92
	3	0.16	0.40	0.95
	5	0.13	0.36	0.96
	8	0.06	0.25	0.98
	31	0.04	0.21	0.98

data points which necessitated a nonzero value of K_s in Eq. [15] to fit the data obtained in the presence of methanol and acetone (see Fig. 7). Thus Eq. [15] in these cases should be regarded as providing a good fit but not necessarily as reflecting the high H_2O_2 coverage of active sites which would correspond to the high K_s values reported in Table 4. It must indeed be stressed that the introduction of the $K_s[H_2O_2]/[S]$ factor in the denominator of Eq. [15] is a mere fitting procedure. The deviations of r_{10} and r_{20} experimental values from the predictions of Eq. [12] reflect internal diffusion limitations and not the effect of solvation on H_2O_2 adsorption equilibrium suggested by Eq. [13].

In all other cases, namely with acetonitrile and water as the solvent and also at low H_2O_2 concentration with methanol and acetone, the initial rate data are essentially free of internal mass transfer limitation. Equation [12], which is observed in these cases, is thus a correct expression for the rate of the rate limiting surface process. According to our kinetic model this process is depicted by Eq. [7] and involves the second adsorption of H_2O_2 on the active site.

Temperature Effect and Activation Energy

Partial oxidation of *n*-hexane at different temperatures (35–65°C) was also investigated and the results are shown in Table 6. From Table 6, it is seen that the conversion of *n*-hexane after 8 h of reaction increases with reaction temperature. The ratio of OL/ONE, however, decreases as the temperature is increased. These experiments were conducted in absence of any added co-solvent, and in these conditions the initial rate is well represented by Eq. [12]:

$$r_{i0} = k_i[H_2O_2]_0^2. \qquad [12]$$

Thus applying the Arrhenius equation

$$k_i = A_i e^{-E_i/RT} \qquad [19]$$

the activation energies and frequency factors can be estimated by linear regression of

$$\ln \frac{r_{io}}{[H_2O_2]_0^2} = \ln A_i - \frac{E_i}{RT}. \qquad [20]$$

The values of A_i and E_i are listed in Table 7. As the rate limiting step is the second H_2O_2 adsorption process depicted by reaction [7], the activation energies found should have the meaning of a heat adsorption of H_2O_2 and the same activation energy should therefore be observed for the 2-hexanol and 3-hexanol formation. Indeed, the two estimates are within 3%. The correlation coeffi-

TABLE 6

Effect of Temperature

Temp. (°C)	*n*-C_6 conversion (mol. %)	H_2O_2 (%)		Product distribution (%)				OL/ONE ratio	2- /3- ratio
		Conv.	Sel.	2OL	2ONE	3OL	3ONE		
35	0.5	13.1	15.8	11.5	34	43.5	11	1.22	0.83
45	1.0	20.4	20.6	9.1	36.9	38.8	15.1	0.92	0.85
55	1.8	27.8	21.2	8.5	38.8	33.5	19.1	0.73	0.81
65	2.2	44.7	22.5	6	43.7	21.3	29	0.38	0.99

Note. Reaction conditions: TS-2, 500 mg; *n*-hexane (mol)/H_2O_2 (mol): 2.7; reaction temperature, 35–65°C; reaction time, 8 h; no co-solvents.

TABLE 7

Activation Energies for *n*-Hexanol Production Rates

	Activation energy (cal/mol) ($\times 10^{-3}$)	Pre-exponential factor A ($ml^2\ mol^{-1}\ h^{-1}$) ($\times 10^{-6}$)	R square
2-OL	9.42	9.07	0.92
3-OL	9.13	6.45	0.93

cients are only in the 0.92–0.93 range corresponding to a possible decrease in the slope of the Arrhenius plot at the higher temperature. This may indicate a significant effect of internal diffusion at 55–65°C in these conditions.

CONCLUSIONS

The most general conclusion of our kinetic analysis of *n*-hexane oxyfunctionalization is related to the experimental fact that whenever the observed data are free from internal diffusion limitations, the initial rates of *n*-hexanol formation are of second order with respect to H_2O_2 and zero order with respect to *n*-hexane (Eq. [12]). This result is shown to be consistent with a rate limiting step involving the second H_2O_2 adsorption on the active Ti site (Eq. [7]). This raises the question of the actual structure of the active site which should allow for simultaneous adsorption of two H_2O_2 molecules.

Interestingly the field of aqueous Ti^{IV} solutions may provide some clues since addition of H_2O_2 to such solutions yields a bright orange colour complex which is believed to correspond to the monomeric $[Ti(O_2)(OH)]^+$ form only at very low pH. For less acidic solutions the peroxohydrate complexes formed are believed to be polymeric forms (32). For example an orange colour is obtained for the dinuclear dipicolinate complex where Ti is bipyramidal pentacoordinate (33):

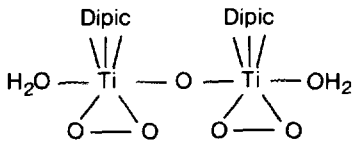

When H_2O_2 is adsorbed on titanium silicalites a bright yellow colour is observed, suggesting a resemblance between the surface species formed and the polynuclear titanium peroxohydrate complexes. In our EXAFS study of the titanium environment in TS-2 (23, 34, 35) it was made clear that at Ti/Ti + Si below 2%, the tetrahedral titanium is mostly present under the form of dimers representing defective structures in the silicalite lattice:

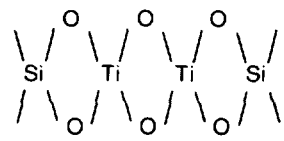

It is therefore suggested that most of the active sites in *n*-hexane oxyfunctionalization would be the complex structure obtained by adsorption of two H_2O_2 molecules on this dimer.

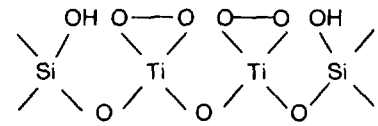

This, however, does not exclude the possibility that isolated tetrahedral Ti may also be an active site. In this case, however, the surface complex formed upon adsorption of H_2O_2 would have to be a diperoxo titanate-like species akin to the recently discovered $[Ti(O_2)_2F_2]^{2-}$ complex ions (36).

Whatever the exact structure of the active site, our kinetic model suggests that the formation of the second peroxo species is the rate limiting step in the primary hydroxylation of *n*-hexane.

ACKNOWLEDGMENTS

We thank professor L. Bonneviot for interesting discussions, Mr. G. Lemay for technical help, and the FCAR fund (programme d'actions spontanées) for financial support.

REFERENCES

1. Rouchaud, J., Sondengam, L., and Fripiat, J. J., *Bull. Soc. Chim. Fr.* **11**, 4387 (1968).
2. Centi, G., and Trifiro. F., *Prepr.—Am. Chem. Soc., Div. Pet. Chem*, **32**(3–4), 754, 1987.
3. Lyons, J. E., *Appl. Ind. Catal. 1983–1984* **3**, 131 (1984).
4. Neumann, R., and Abu-Gnim, C., *J. Chem. Soc., Chem. Commun.*, 1324 (1989).
5. Perego, G., Bellussi, G. Corno, C., Taramasso, M., Buonuomo, F., and Esposito, A., *in* "Proceedings, 7th International Conference on Zeolites, Tokyo 1986" (Y. Murakami, A. Iijima, and J. W. Ward, Eds.), p. 129. Kodansha–Elsevier, Amsterdam, 1987.
6. Esposito, A., Taramasso, M., Neri, C., and Buonomo, F., U.K. Patent 2,116,974 (1985).
7. Notari, B., *in* "Innovation in Zeolite Material Science" (P. J. Grobet, W. J. Mortier, E. P. Vansant, and G. Schulz-Ekloff, Eds.), Studies in Surface Science and Catalysis, Vol. 37, p. 413, Elsevier, Amsterdam, 1987.
8. Thangaraj, A., Kumar, R., and Ratnasamy, P., *Appl. Catal.* **57**, L1 (1990).
9. Tuel, A., Moussa-Khouzami, S., Ben Taarit, Y., and Naccache, C., *J. Mol. Catal.* **68**, 45 (1991).

10. Neri, C., Esposito, A., Anfossi, B., and Buonomo, F., Eur. Patent 100119 (1984); Neri, C., Anfossi, B., and Buonomo, F., Eur. Patent 100118 (1984).
11. Clerici, M. G., Bellussi, G., and Romano, U., *J. Catal.* **129,** 159 (1991).
12. Romano, U., Esposito, A., Maspero, F., Neri, C., and Clerici, M. G., *Chim. Ind. (Milan)* **72**(7), 610 (1990).
13. Esposito, A., Neri, C., and Buonomo, F., It. Pat. Appl. 22607, A/82.
14. Esposito, A., Taramasso, M., Neri, C., and Buonomo, F., U.K. Patent 2,116,974 (1983).
15. Huybrechts, D. R. C., De Bruycker, L., and Jacobs, P. A., *Nature* **345,** 240 (1990).
16. Tatsumi, T., Nakamura, M., Negishi, S., and Tominaga, H., *J. Chem. Soc., Chem. Commun.*, 476 (1990).
17. Reddy, J. S., Sivasanker, S., and Ratnasamy, P., *J. Mol. Catal.* **70,** 335 (1991).
18. Clerici, M. G., *Appl. Catal.* **68,** 249 (1991).
19. Parton, R. F., Huybrechts, D. R. C., Buskens, Ph., and Jacobs, P. A., *in* "Catalysis and Adsorption by Zeolites" (G. Ohlmann *et al.*, Eds.), Studies in Surface Science and Catalysis, Vol. 65, p. 47. Elsevier, Amsterdam, 1991.
20. Huybrechts, D. R. C., Buskens, P. L., and Jacobs, P. A., *J. Mol. Catal.* **71,** 129 (1992).
21. Thangaraj, A., Kumar, R., Mirajkar, S. P., and Ratnasamy, P., *J. Catal.* **130,** 1 (1991).
22. Furniss, B. S., Hannaford, A. J., Rogers, V., Smith, P. W. G., and Tatchell, A. R., "Vogel's Textbook of Practical Organic Chemistry Including Qualitative Organic Analysis," p. 334. Wiley, New York, 1978.
23. Bittar, A., Trong On, D., Bonneviot, L., Kaliaguine, S., and Sayari, A., *in* "Proceedings of the Ninth International Zeolite Conference" (R. von Ballmoos, J. B. Higgins, and M. M. J. Treacy, Eds.), p. 453. Butterworth–Heinemann, Boston, 1993.
24. Tuel, A., Ben Taarit, Y., Lemay, G., Adnot, A., and Kaliaguine, S., *Appl. Catal.*, in press.
25. Fu, H., "Co-Solvent Effect in Oxyfunctionalization of *n*-Hexane by H_2O_2 on TS-2." MSc thesis, Université Laval, Québec, 1994.
26. Polak, J., and Lu, B. C. Y., *Can. J. Chem.* **51,** 4018 (1973).
27. Groves, F. R. Jr., *Environ. Sci. Technol.* **22**(3), 282 (1988).
28. El-Zoobi, M. A., Ruch, G. E., and Groves, F. R. Jr., *Environ. Sci. Technol.* **24**(9), 1332 (1990).
29. van der Pol, A. J. H. P., Verduyn, A. J., and van Hooff, J. H. C., *Appl. Catal.* **92,** 113 (1992).
30. Levenspiel, O., (Ed.), "Chemical Reaction Engineering," (p. 469. Wiley, New York, 1972.
31. Wu, P., Debebe, A., and Ma, Y. H., *Zeolites* **3,** 118 (1983).
32. Cotton, F. A., and Wilkinson, G., "Advanced Inorganic Chemistry," p. 659. Wiley, New York 1988.
33. Schwarzenbach, D., *Helv. Chim. Acta* **55,** 2990 (1972).
34. Trong On, D., Bittar, A., Sayari, A., Kaliaguine, S., and Bonneviot, L., *Catal. Lett.* **16,** 85 (1992).
35. Trong On, D., Bonneviot, L., Bittar, A., Sayari, A., and Kaliaguine, S., *J. Mol. Catal.* **74,** 233 (1992).
36. Chaudhuri, M. K., and Das B., *Inorg. Chem.* **25,** 168 (1986).